Title
Unique f-level resonant state within the gap in Ce3Au3Sb4 single crystals: Magnetic, thermal, and transport properties

Journal
Physical Review B, 76(15)

ISSN
2469-9950

Authors
Lee, Han-Oh
Jo, Youn-Jung
Balicas, Luis
et al.

Publication Date
2007-10-15

DOI
10.1103/physrevb.76.155204

Unique *f*-level resonant state within the gap in $Ce_3Au_3Sb_4$ single crystals: Magnetic, thermal, and transport properties

Han-Oh Lee,[1,2] Youn-Jung Jo,[3] Luis Balicas,[3] P. Schlottmann,[3,4] Cathie L. Condron,[5] V. A. Sidorov,[2,6] Peter Klavins,[1] Susan M. Kauzlarich,[5] J. D. Thompson,[2] and Z. Fisk[1,7]

[1]*Department of Physics, One Shields Avenue, University of California, Davis, California 95616, USA*

[2]*Los Alamos National Laboratory, Los Alamos, New Mexico 87545, USA*

[3]*National High Magnetic Field Laboratory, Florida State University, Tallahassee, Florida 32310, USA*

[4]*Department of Physics, Florida State University, Tallahassee, Florida 32306, USA*

[5]*Department of Chemistry, One Shields Avenue, University of California, Davis, California 95616, USA*

[6]*Vereshchagin Institute for High Pressure Physics, Russian Academy of Sciences, 142190 Troitsk, Russia*

[7]*Department of Physics and Astronomy, 4129 Frederick Reines Hall, University of California, Irvine, California 92697-4575, USA*

(Received 29 May 2007; published 3 October 2007)

The magnetic, thermal, and transport properties of single crystals of the narrow gap semiconductor $Ce_3Au_3Sb_4$ have been studied. Transport data are consistent with an exponential activation and variable range hopping at low temperatures, which is characteristic of weak disorder and localization. The specific heat and the magnetic susceptibility data suggest the existence of a large density of states of localized states in the gap. The physics is then different from standard Kondo insulators. From its unique physical properties, we propose a three band model (valence, conduction, and *f* bands) with weak disorder that explains most of the experimental findings.

DOI: 10.1103/PhysRevB.76.155204 PACS number(s): 72.20.−i, 71.27.+a, 72.15.Rn, 72.80.Sk

I. INTRODUCTION

The Kondo effect that occurs in rare earth and actinide intermetallic systems has been intensively studied due to its interesting features associated with a variety of the ground states.[1] Although it usually occurs in metallic systems, there are small gap semiconductors with strong *f*-electron correlations, known as Kondo insulators.[2] Examples of these materials include SmB_6, CeNiSn, $Ce_3Bi_3Pt_4$, and $Ce_3Pt_3Sb_4$.[2–6] These compounds commonly have a valence fluctuating or intermediate valence character of the *f* sites due to strong hybridization of the *f* electron with the conduction band, which is responsible for the gap at the Fermi level.[7]

$Ce_3Au_3Sb_4$, which has the same crystal structure as $Ce_3Pt_3Sb_4$ and $Ce_3Pt_3Bi_4$, on the other hand, is an exception in that it shows semiconducting behavior in its transport properties, but the *f* moment is well localized, which means that the hybridization of the *f* moment with the conduction electrons cannot be the only origin of the semiconducting behavior.[6–11] Since $La_3Au_3Sb_4$ and $Pr_3Au_3Sb_4$ also show semiconducting gaps, according to optical measurements and a band structure calculation for $La_3Au_3Sb_4$,[12–14] it has been suggested that the observed gapped behavior in $Ce_3Au_3Sb_4$ is due to a normal band gap. Surprisingly, $Ce_3Au_3Sb_4$ reveals a large specific heat coefficient, $C/T=\gamma$, at low temperature. γ is proportional to the density of states at the Fermi level. The question is then what is the origin of this large density of states in a (insulating) system with very low carrier density. There is a broad peak around 0.8 K in the specific heat that resembles a single ion Kondo resonance. Furthermore, the magnetic field dependence of the peak in the specific heat behaves as expected for a single ion Kondo system.[9]

However, Amato *et al.* observed a dramatic increase of the muon spin resonance relaxation rate below 2.5 K and suggested a possible spin glass state.[15,16] A different scenario, that of a zero-gap semimetal, has been proposed by Broderick *et al.* from measurements of a metallic thermoelectric power and nonactivated behavior of the resistivity in their samples.[17] In contrast, usual Kondo lattice behavior and magnetic ordering at 5 K were reported in Ref. 10. The origin of these controversial results is most likely the strong sample dependence, possibly due to a deficiency on the Sb sites. The metallic thermoelectric power, however, is found to be deficiency independent, in contrast to the observed semiconducting behavior in the resistivity.

These previous studies on $Ce_3Au_3Sb_4$ have been performed with polycrystalline samples. In order to verify this unusual behavior of $Ce_3Au_3Sb_4$, we have grown single crystals and studied them through magnetic susceptibility, resistivity, specific heat, magnetoresistance, and high pressure experiments. The specific heat of $(Ce_{1-x}La_x)_3Au_3Sb_4$ crystals is also presented. Overall, our experimental results agree well with the polycrystalline data previously reported, except for the resistivity data, which are strongly sample dependent.

From our experimental results, we assume that the semiconducting behavior in $Ce_3Au_3Sb_4$ arises from three types of states, namely, a valence band, a conduction band, and a hybridized *f* band. This differs from the usual picture of a hybridization gap which requires only two bands. The *f* band is very narrow and lies in the gap, and hence, weak disorder can localize the *f*-like states. Consequently, the transport properties are semiconductorlike, but due to disorder, they can be strongly sample dependent. The *f* band also provides the necessary density of states at the Fermi level to explain the large C/T at low temperature. We will discuss similar semiconducting systems with large C/T and compare them with $Ce_3Au_3Sb_4$.

II. EXPERIMENT

$Ce_3Au_3Sb_4$ single crystals were synthesized using excess Au and Sb flux. The starting materials used are high purity

TABLE I. Space group I-43*d*, $a=10.0029(12)$ Å, $Z=4$, $R1=0.0262$, $wR2=0.0502$, and extinction coefficient of 0.00141(10). Largest difference peak and hole=1.324 and −1.191 e Å^{-3}. 211 reflections, zero restraints, and 11 parameters were used for the refinement. U_{eq} is defined as one-third of the trace of the orthogonalized U^{ij} tensor. When the site occupancies for each atom were allowed to refine, there was no significant deviation from fully occupied and were, accordingly, fixed to full for the remainder of the refinement procedures.

Atom	x	y	z	U_{eq}	Occupancy
Ce	0.375	0	0.25	0.0015(5)	1
Au	0.875	0	0.25	0.0026(4)	1
Sb	0.08533(9)	0.08533(9)	0.008533(9)	0.0017(5)	1

Ce (AMES, 4*N*), Au (5*N*), and Sb (5*N*). The constituent elements were placed in an alumina crucible and sealed in an evacuated quartz tube. The ampoule was then heated to 1150 °C followed by slow cooling down to 500 °C before spinning the reaction to separate the crystals from the molten flux. Single-crystal $La_3Au_3Sb_4$ has also been synthesized using the same method in order to compare it with $Ce_3Au_3Sb_4$. Single-crystal x-ray diffraction patterns were collected on an R3m/V Siemens diffractometer, equipped with a graphite monochromator and a modified Enraf-Nonius low-temperature apparatus, by using Mo $K\alpha$ radiation with $\lambda = 0.710\,73$ Å. A suitable crystal of dimensions $0.3\times0.4\times0.2$ mm^3 was fixed to a quartz fiber with epoxy, centered, and indexed. The ψ-scan method was used to perform an empirical absorption correction. The structure was identified by direct methods and refined by the full-matrix least-squares method on F^2.[18] The magnetic moment was measured with a commercial Quantum Design magnetic property measurement systerm (MPMS). The heat capacity was measured to ^{3}He temperatures in a Quantum Design physical property measurement system (PPMS) using the relaxation time technique. The dc electrical resistivity was obtained by the standard four-probe method using a PPMS down to 0.36 K. The systematic measurement of the electrical resistance under magnetic fields up to 33 T along a direction perpendicular to the current and in the temperature range between 1 and 50 K was performed with a lock-in technique in a Bitter magnet coupled to a ^{3}He cryostat. The electrical resistivity was measured under hydrostatic pressure using both a Be/Cu piston-cylinder clamp device and a toroidal anvil clamp device. The latter is the profiled anvils system supplied with an alumina-epoxy gasket and Teflon capsule, containing pressure-transmitting liquid, sample, and pressure sensor. The pressure was determined from the variation of the superconducting transition of lead using the pressure scale of Eiling and Schilling.[19] The width of the Pb transition implied a pressure gradient of 0.5 kbar at the highest pressure. The resistivity under pressure was measured with a standard four-probe technique using an LR-700 Linear Research bridge operating at an applied current of 10 μA–1 mA depending on the temperature range.

We noted that crystalline $Ce_3Au_3Sb_4$ is very sensitive to extrinsic conditions. When the sample was polished with alumina polishing paper, the resistivity exhibited metallic, Kondo-lattice-like behavior as a function of temperature. This extreme sensitivity may be due to strain dependence of surface states because of the intrinsic narrow gap. Surface sensitivity to polishing has been reported in SmS (Refs. 20 and 21) and $CeRhIn_5$,[22] although their physics are different. All the samples used for resistivity measurements thus were not polished but were cut with a razor blade or used of natural habit (pressure experiment). Pt wires were attached on the fresh cut surfaces with silver epoxy, followed by moderate heat treatment for not more than 15–20 min to cure the epoxy because long time exposure to heat also degraded the sample to be metallic. Spot welding is difficult on this material because of the intrinsic insulating character of $Ce_3Au_3Sb_4$. Due to the dendritic sample shape and the way samples were prepared for resistivity measurement, error bars for the absolute value of the resistivity are larger than for more typical well-defined geometries. Crystals used for the transport experiments under high pressure and magnetic fields were different from the sample for ambient pressure zero-field data, which yields slightly different absolute values for the resistivity and the activation gap.

III. RESULTS

Single-crystal x-ray diffraction was preformed in order to confirm the crystal structure and check for vacancy formation in $Ce_3Au_3Sb_4$ single crystals. All pertinent information of the final refinement details, including fractional coordinates, is given in Table I. Refinement results confirmed that $Ce_3Au_3Sb_4$ crystallizes in the cubic crystal system with space group I-43*d* and a lattice constant of 10.0229(12) Å. When the site occupancies for each atom were allowed to refine, there was no significant deviation from fully occupied. Therefore, according to our single-crystal x-ray refinement, there is no indication of any crystallographic site being deficient.

An important feature of this structure is that each Ce atom is surrounded by four Au atoms forming a distorted tetrahedron, making the symmetry of the Ce site tetragonal so that the six degenerate Ce^{3+} states are split into three doublets by the influence of the crystalline electric field (see Fig. 1).

Figure 2(a) shows the temperature dependence of the magnetic susceptibility. No magnetic phase transition is observed down to 1.8 K. A Curie-Weiss fit of the inverse susceptibility above 50 K [see inset in Fig. 2(a)] yields an effective moment of $2.38\mu_B$ and a Weiss temperature of −7 K, indicative of a localized Ce^{3+} ($=2.54\mu_B$) state with small antiferromagnetic correlations. The slight curvature below

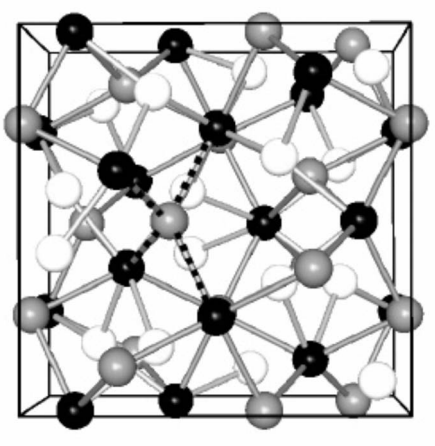

FIG. 1. Illustration of the cubic unit cell for $Ce_3Au_3Sb_4$, Ce (gray), Au (black), and Sb (white); the dotted lines indicate the tetrahedral environment of the Ce atom.

25 K is the consequence of the crystalline electric field which reduces the effective moment from that of the sixfold degenerate states of the free Ce^{3+}-ion to that of the doubly degenerate ground state. The magnetization as a function of the magnetic field [Fig. 2(b)] tends to saturate at high fields at a value slightly larger than $1.1\mu_B$ at 7 T. The fit to a Brillouin function for $S=1/2$ with a z component of the spin $1.258\mu_B$ is satisfactory, suggesting that the ground state is most likely a tetragonal $\Gamma_7^{(2)}$ doublet state. The magnetic data presented here agree well with the reported data on a polycrystalline sample.[6]

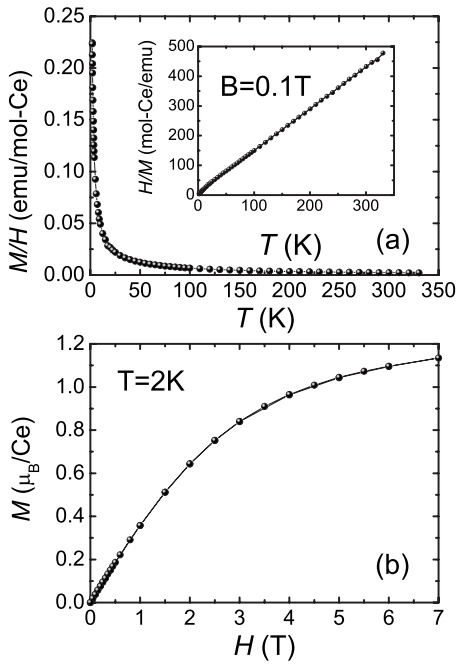

FIG. 2. (a) Magnetic susceptibility as a function of temperature under applied magnetic field of 0.1 T. (Inset) Inverse susceptibility versus temperature. (b) Magnetization in units of μ_B as a function of magnetic field.

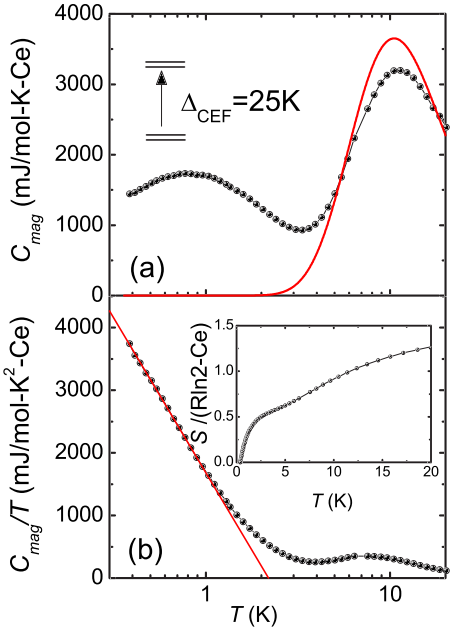

FIG. 3. (Color online) (a) Magnetic contribution to the specific heat, obtained by subtracting the corresponding specific heat of $La_3Au_3Sb_4$, as a function of temperature. The red curve is a fit to the Schottky specific heat for two doublet states separated by 25 K (Δ_{CEF}). (b) Magnetic specific heat divided by the temperature versus temperature. The red line is a guide to the eye to show the logarithmic temperature dependence. (Inset) Entropy in units of $R\ln 2$ versus the temperature.

The temperature dependence of the magnetic part of the specific heat is displayed in Fig. 3(a). The magnetic contribution to the specific heat is obtained by subtracting the specific heat of $La_3Au_3Sb_4$ to remove the phonon contribution and, in this way, isolate the magnetic contribution. The broad peak at about 12 K is most likely due to the first excited crystalline field doublet, as also suggested by the susceptibility data. The corresponding entropy [inset of Fig. 3(b)] is about $0.6R\ln 2$ at 5 K, implying a doubly degenerate ground state. The red curve in Fig. 3(a) represents the fit to a crystal field Schottky specific heat of two doublets separated by 25 K. Another broad peak appears below 3 K, which is similar to that expected for a single ion Kondo effect. If assumed to be a single impurity Kondo effect, the corresponding Kondo temperature is estimated to be ~1.85 K. The origin of this broad peak, however, is not clear, i.e., whether it is due to a Kondo resonance or arises from some other magnetic contribution. The specific heat divided by temperature presented in Fig. 3(b) increases as T is lowered and reaches 3.8 J/mol K^2 at 0.38 K. Note that C_m/T has a logarithmic temperature dependence below 1 K, which could arise either from a diverging density of states near the Fermi level or many body effects (quantum criticality or interactions between f electrons). The Sommerfeld coefficient γ from the specific heat measurement of $La_3Au_3Sb_4$ is 0.4 mJ/mol K^2 (not shown here), which is consistent with the polycrystalline result.[6] This rather small γ value implies a small density of states, as expected from a small number of carriers in the system. Previous Hall constant measurements[6,8] on polycrys-

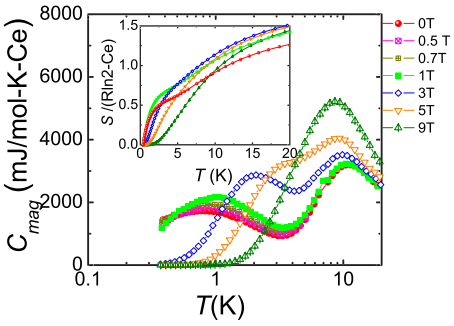

FIG. 4. (Color online) Magnetic contribution to the specific heat versus temperature for various magnetic fields. (Inset) Entropy as a function of the temperature for the same magnetic fields.

talline samples of $Ce_3Au_3Sb_4$ indicate that $Ce_3Au_3Sb_4$ could also be a low carrier density system. The question is then what is the origin of the large density of states in this low carrier density system.

To clarify the nature of the low-temperature specific heat peak around 1 K, we measured the specific heat in an applied magnetic field (see Fig. 4). The behavior is essentially the same as the data published by Kasaya *et al.*,[9] after subtracting the Schottky peak due to a crystal field splitting of 25 K. The increasing peak intensity with field, as well as the peak position moving toward higher temperature, is a trend expected from the Kondo effect. The entropy at 20 K in 5 T is $0.25R \ln 2$ larger than the entropy in a 0 T field. There is a considerable amount of hidden entropy below 0.38 K, which can be estimated as $\sim 0.2R \ln 2$ by linearly extrapolating the low-temperature zero-field entropy to zero temperature. The entropy is low compared to $R \ln 2$ for a doublet ground state at 5 K or $R \ln 4$ if the first excited state is included at 20–25 K.

The specific heat of La-diluted samples (La substituting for Ce) is presented in Fig. 5. The peak around 12 K does not change, meaning that the crystalline field splitting is independent of La dilution. The position of the low-temperature peak moves to lower temperatures except for $x=0.38$ as the La concentration increases, which is an indication that the low-energy scale becomes smaller.

The resistivity data are puzzling and very sample dependent. Unlike the susceptibility and the specific heat data,

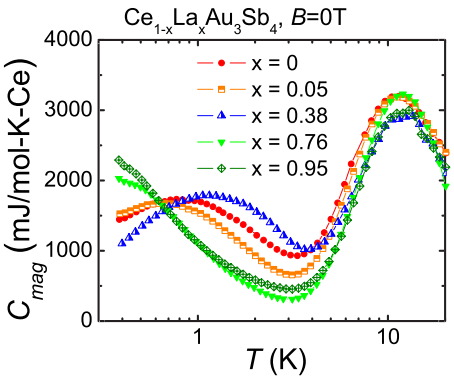

FIG. 5. (Color online) Magnetic contribution to the specific heat as a function of temperature for samples diluted with La.

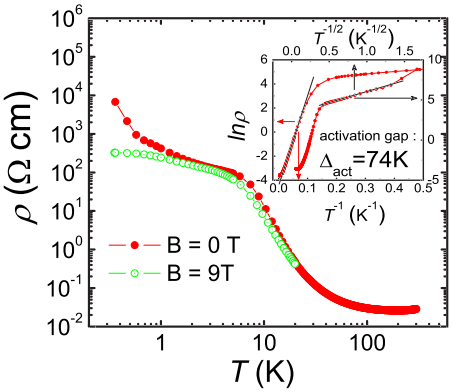

FIG. 6. (Color online) Resistivity as a function of temperature in zero magnetic field (red solid circles) and 9 T (yellow-green open circle). (Inset) ln ρ vs T^{-1} and vs $T^{-1/2}$ showing the activation and variable range hopping behaviors, respectively.

which agree well with polycrystalline data,[6,8,9] the resistivity shows a somewhat different behavior from the previously reported results. The temperature dependence of the resistivity is displayed in Fig. 6. It shows slightly metallic behavior down to 150 K and insulating behavior at lower temperatures. Our best sample shows a resistance ratio of 5×10^5 at 0.36 K from its room temperature value, which confirms the insulating nature of this compound. The trend to saturate below 10 K is probably due to states within the gap. The activated behavior for the temperature range between 20 and 80 K has an activation gap of 50–100 K depending on the sample, suggesting the existence of a small transport energy gap (inset in Fig. 6). On the other hand, for the temperature range between 0.5 and 5 K (inset of Fig. 6), the data are well fitted by the variable range hopping (VRH) model in the presence of Coulomb interactions, where $\rho(T) = \rho_0 \exp(T_0/T)^{1/2}$, $T_0 \propto [N(E_F)\xi^3]^{-1}$, $N(E_F)$ is density of states at the Fermi level, and ξ is localization length. This implies that a small number of carriers hop between weakly localized states. The weak localization at low T could be caused by disorder or impurities in the system. Considering that $La_3Au_3Sb_4$ is a band insulator[12–14] and that the $4f$ electron of Ce in $Ce_3Au_3Ab_4$ is localized, we assume that $Ce_3Au_3Sb_4$ is also an intrinsic band insulator or narrow gap semiconductor with a gap of 50–100 K and that there is an additional $4f$ state for each Ce ion. Combined with weak disorder, this may lead to weakly localized states. The VRH may also be responsible, at least partially, for the reported[17] metallic thermoelectric power. An applied magnetic field of 9 T changes the resistivity dramatically especially below 0.5 K, but this is also strongly sample dependent.

The magnetoresistance (MR) down to ~1.5 K with applied magnetic fields up to 33 T is shown in Fig. 7. The large negative MR is associated with the closing of the gap. The activation gap decreases from 50 K for zero field to 37 K for 30 T roughly in a linear way for this sample. Extending this line to zero temperature gives an estimated magnetic field of about 110 T to completely close the gap, which is reasonable since 110 T is an energy scale comparable to the size of the gap (50–100 K) at zero field. This mild reduction of the

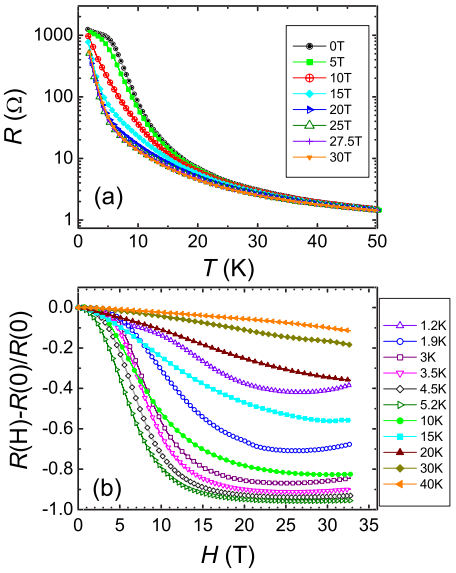

FIG. 7. (Color online) (a) Resistance versus temperature at different magnetic fields. (b) Magnetoresistance versus magnetic field at various temperatures. The large magnetoresistance does not scale with H^2 at low temperatures.

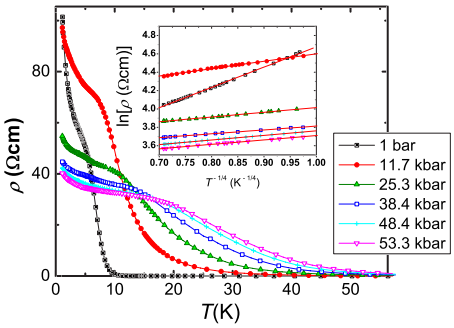

FIG. 8. (Color online) Pressure (P) dependence of the resistivity of $Ce_3Au_3Sb_4$. If fitted to an activation law (although the fit is not very good), the gap clearly increases with pressure as the slopes of $\ln \rho$ vs T^{-1} plot at all T regime above 10 K are enhanced continuously with increasing pressure. The fitting range corresponds to sample resistivity of $\sim 1-5\ \Omega$ cm and gets shifted to higher T with increasing pressure. (Inset) Fit to the VRH model without Coulomb interaction between 1.1 and 4 K. A fit of similar quality can also be made to VRH with Coulomb interaction. The fitting parameters for both activation and VRH fits are displayed in Fig. 9.

activation gap, however, does not seem to be enough to explain the very large negative MR at low temperature in $Ce_3Au_3Sb_4$. The MR is also quite sample dependent. For example, in this sample, a very large negative MR appears in the temperature range of 3–5 K (VRH fits below 3 K in this sample), whereas negative MR is not as pronounced for the sample displayed in Fig. 6. Yet, overall, the negative MR becomes large when the resistivity starts to bend away from the activation behavior below 10 K, which is the border between activated and VRH behaviors. Although it is nominally insulating, there is finite transport in the VRH regime due to hopping processes. If f electrons are involved in this VRH process, magnetic fields will reduce the number of possible states (see Fig. 4 inset for entropy below 10 K) due to Zeeman splitting of the ground doublet and will reduce the scattering rate, causing negative magnetoresistance. The small crystal electric field (CEF) gap (25 K) will make this MR further complicated, and hence, the MR is not as large above $H \sim 20-25$T and/or $T \sim 25$ K. The magnetic field could also help to delocalize the f electron, which would increase the negative MR. The large negative MR at low temperature, thus, suggests that the f electron may participate in the VRH process. The large MR below 1 K in Fig. 6, where the resistivity deviates from VRH behavior, should have different physics from VRH and is not understood at this point. The T range for VRH decreases toward lower T when magnetic fields are applied and VRH behavior is not obvious above 15 T. The Zeeman splitting of the ground and/or first excited crystal-field states (0 and 25 K) of the f moment should be responsible for this change in VRH behavior. A fit of ρ(T) to VRH in this small T region for 9 T gives a value of T_0 that is reduced to $\sim$70% of its zero-field value. This thus suggests that the in-gap state is delocalized under magnetic field due to Zeeman splitting of f states, in addition to the reduction of the activation gap. The usual H^2 dependence of MR appears for small fields above 10 K, but no such scaling behavior was observed below 5 K, as demonstrated in Fig. 7(b). The MR of the sample of Fig. 6, however, follows the H^2 behavior between 1 and 3 K for magnetic fields up to 1 T.

In Fig. 8, we present the pressure dependent resistivity data. The resistivity at finite pressures can be fitted with an activation law at limited temperature range and with VRH (see the inset of Fig. 8) below 4–5 K. For this sample, the activation gap (Δ_{act}), extracted from the data, is enhanced from 90 to 270 K with increasing pressure from 1 bar to 53.3 kbar. This behavior of increasing activation gaps under pressure is similar to the pressure dependence of the gap in the well-known Kondo insulator $Ce_3Pt_3Bi_4$, which has a resistivity value that is 3 orders smaller than $Ce_3Au_3Sb_4$ at low temperature. Since isostructural mixed valence system $Ce_3Pt_3Sb_4$ has a smaller lattice constant and a larger gap that derives, in part, from f-ligand hybridization, it may not be surprising to see that pressure enhances the insulating gap in $Ce_3Au_3Sb_4$. In general, the hybridization of the Ce f electron with ligand-atom states increases with pressure, and hence, an increase of the gap is expected for Ce-based Kondo insulator. For the low T range below 4–5 K, we have fitted the resistivity of $Ce_3Au_3Sb_4$ to VRH with or without Coulomb interactions between pinned disorder sites (see the inset of Fig. 8). It is not clear which fit is better. In the inset of Fig. 6, we show the fit of the ambient pressure data to VRH with Coulomb interaction $[\rho(T) = \rho_0 \exp(T_0/T)^{1/2}]$, while in the inset of Fig. 8, the resistivity under pressure is fitted to the VRH model without Coulomb interaction $[\rho(T) = \rho_0 \exp(T_0/T)^{1/4}]$. Inspection of these data and their analysis show that the activation gap increases with pressure, but ρ_0 and T_0 decrease with applied pressure, the latter by 2 orders of magnitude. VRH (without Coulomb interaction) in transport under pressure in a Kondo insulator has been observed in $Ce_3Pt_3Bi_4$ by Cooley *et al.*,[23] who suggest that in-gap states develop in the hybridization gap under

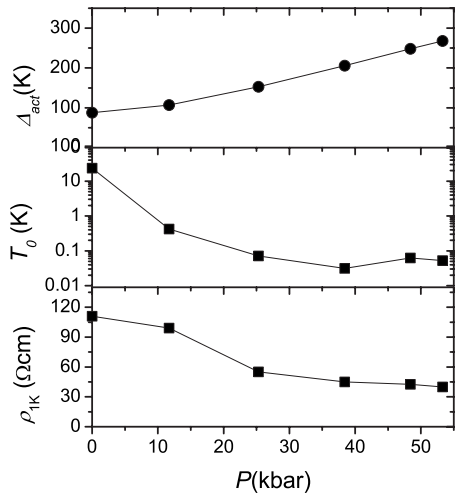

FIG. 9. Parameters of the fits of the resistivity vs temperature as a function of applied hydrostatic pressure. The activation gap is shown in the top panel, while the middle and lower panels refer to the VRH fits. Here, Δ_{act} denotes activation gap, T_0 is a parameter of VRH fit, which is inversely proportional to density of state $[N(E_F)]$ and cube of localization length (ξ), and ρ_{1K} means resistivity value at 1 K.

pressure. The pressure dependence of $Ce_3Au_3Sb_4$ is very similar to that of $Ce_3Pt_3Bi_4$ (see Ref. 23). In both cases, the activation gap increases and ρ_0 decreases with pressure. The main difference is in T_0, which increases by 2 orders of magnitude in $Ce_3Bi_4Pt_3$ but decreases by 2 orders of magnitude in $Ce_3Au_3Sb_4$ (see Fig. 9).

A different pressure dependence for $Ce_3Bi_4Pt_3$ has been reported in Ref. 24, where the measurements are performed under more nearly hydrostatic condition. Hence, it is more appropriate to compare our hydrostatic pressure data for $Ce_3Au_3Sb_4$ with that of Ref. 24 for $Ce_3Bi_4Pt_3$. ρ_0 and T_0 increase under pressure in Ref. 24, which is the opposite result from our VRH fit for $Ce_3Au_3Sb_4$. This increase indicates that the states within the gap of $Ce_3Bi_4Pt_3$ are more localized as the insulating gap increases. T_0 here is inversely proportional to the cube of the localization length (ξ) of the impurity state wave function. A decrease of T_0 in $Ce_3Au_3Sb_4$ therefore means an enhancement of ξ, indicating that the states are more delocalized at higher pressure. At a first glance, this appears to conflict with the increase of the insulating gap. However, if we assume that the strength of the hybridization between localized f electron and the conduction electrons is enhanced with pressure, then the in-gap states, which have predominantly f character, will broaden and delocalize further, lowering the low T resistivity (ρ_0) as well as T_0. This is consistent with the present data. In contrast, in $Ce_3Bi_4Pt_3$, the hybridization between f- and conduction electron appears not to be necessarily related to the hopping between impurity states within the gap. Hence, this pressure experiment provides insight into the different origins of the gap and the in-gap states between these two compounds.

IV. DISCUSSION

A key question now is what is the origin of the large C/T at low temperatures in a low carrier density system. If the system were metallic, it might simply be explained by the Kondo resonance. Based on the low-temperature resistivity data, we assume that small disorder in the system causes localization of f states in the gap and pins the Fermi level. As discussed above, this could give rise to VRH transport at low temperatures. Furthermore, hybridization of the f states with the valence and conduction bands can lead to a broadening of the f band. This can explain simultaneously the localized moment behavior of Ce^{3+} in the susceptibility and the large specific heat Sommerfeld coefficient within the scheme of an insulating band picture. In other words, the apparent divergence of the specific heat coefficient is not caused by many conduction electrons at the Fermi surface but rather by a large and narrow density of localized f states.

Although $Ce_3Au_3Sb_4$ is a stoichiometric compound, an inevitable small amount of disorder in the system breaks the translational symmetry. Hence, unlike in a usual metallic Kondo lattice, there is no coherent scattering at low temperatures. We consider three bands, namely, a valence band, a conduction band, and an f-electron band within the gap. The gap between the valence and conduction bands, already present in $La_3Au_3Sb_4$, is taken to be 50–100 K and the f-level width should be a few Kelvin. The Hamiltonian can be written as follows:

$$\mathrm{H} = \sum_{\vec{k},\sigma} [\varepsilon_{1\vec{k}} C^{+}_{1\vec{k}\sigma} C_{1\vec{k}\sigma} + \varepsilon_{2\vec{k}} C^{+}_{2\vec{k}\sigma} C_{2\vec{k}\sigma} + \tilde{\varepsilon}_f f^{+}_{\vec{k}\sigma} f_{\vec{k}\sigma} + V_1 (C^{+}_{1\vec{k}\sigma} f_{\vec{k}\sigma} + f^{+}_{\vec{k}\sigma} C_{1\vec{k}\sigma}) + V_2 (C^{+}_{2\vec{k}\sigma} f_{\vec{k}\sigma} + f^{+}_{\vec{k}\sigma} C_{2\vec{k}\sigma})],$$

where the $\varepsilon_{1\vec{k}}$, $\varepsilon_{2\vec{k}}$ and $\tilde{\varepsilon}_f$ are the energy dispersions of the valence, conduction, and f bands, respectively, and V_1 and V_2 are the hybridization strengths between local f electrons and the valence and conduction band electrons, respectively. We write $\varepsilon_{1\vec{k}} = -\Delta_1 - \varepsilon_{\vec{k}}$, $\varepsilon_{2\vec{k}} = \Delta_2 + \varepsilon_{\vec{k}}$, and $\tilde{\varepsilon}_f = \varepsilon_f + \frac{1}{2} U n_f + \Sigma_U(\varepsilon)$, where the self-energy due to the Coulomb repulsion inside the gap is $\Sigma_U(\varepsilon) = (\gamma^* - 1)\varepsilon$ (the real part is linear in the energy, the imaginary part vanishes due to the gap, and γ^* is inversely proportional to the Kondo renormalization). Here, $\varepsilon_{\vec{k}}$ varies in the interval, $[0, D]$ where D is the band cutoff energy. The band edges of the valence and conduction bands are at Δ_1 and Δ_2, respectively. In the absence of hybridization, the gap between the valence and conduction bands is then $\Delta_1 + \Delta_2$. The diagonalization of the 3×3 matrix of the Hamiltonian yields the dispersions and hence the density of states. The simplest situation corresponds to $\Delta_1 = \Delta_2 = \Delta$, $\varepsilon_f + \frac{1}{2} U n_f = 0$, and $V_1 = V_2 = V$. For this symmetric case, the energy eigenvalues are $\varepsilon = 0$ and $\varepsilon = \pm \sqrt{(\varepsilon_{\vec{k}} + \Delta)^2 + 2V^2 / \gamma^*}$, indicating a renormalization of the gap due to the hybridization (of the order of the Kondo temperature) and a delta-function-like f state pinning the Fermi level. Asymmetries in the model parameters introduce a dispersion and a very small width to the f states in the gap. Due to their quasilocalized nature, these states are strongly affected by disorder. Even very weak disorder will broaden the f density of states and destroy the mobility (promote localization). The high density

of states will give rise to a large Sommerfeld coefficient while the system is an insulator.

Under applied magnetic field, the gap between the valence and conduction bands is reduced due to the shift of the density of states for the up and down spins in opposite directions as a consequence of the Zeeman effect. The localized f states are also broadened by the magnetic field, so that the MR is expected to be negative.

The above picture is different from normal Kondo insulators in that the gap is not due to the strong hybridization between the local f electron and the conduction band but already exists in the corresponding La-analog compound. Thus, in a Kondo insulator, γ is very small because of the hybridization gap and is usually determined by intrinsic or extrinsic in-gap states. On the other hand, in the present system γ is very large due to the localized f states. Not understood yet is the logarithmic temperature dependence of the specific heat at low T.

Let us assume that the La- and Pr-analog compounds, i.e., $La_3Au_3Sb_4$ and $Pr_3Au_3Sb_4$, are semimetals rather than insulators. This is a possibility due to the strong sample dependence of the resistivity. Our model would give essentially the same results for $Ce_3Au_3Sb_4$, since (in the asymmetric case) the V_1 and V_2 open gaps between the valence and f bands and between the f and the conduction bands. Even weak disorder will still localize the f states. Hence, the results for $Ce_3Au_3Sb_4$ are basically the same if we start from a semimetal rather than insulator.

There are other examples of low carrier semiconductors with large specific heat coefficient.[25] The mixed valence systems, Sm_3X_4 (X=Te, Se), have revealed large γ values of 0.79 and 0.6 J/K^2 mol Sm^{3+}, respectively, with semiconducting resistivity, which is similar to the properties of $Ce_3Au_3Sb_4$.[26,27] However, unlike $Ce_3Au_3Sb_4$, the specific heat anomaly is reduced under applied magnetic fields. μSR experiments[28] suggest spin glass behavior at low temperatures, which is related to the large γ. A homogeneous distribution of Sm^{3+} and Sm^{2+} ions (no superlattices) may be the origin of this spin glass behavior. Since Ce is well localized in $Ce_3Au_3Sb_4$ as well as stoichiometric, glassy behavior is unlikely, although it cannot be ruled out at this point. Neutron scattering experiments (currently under progress) could provide valuable information about the spin configurations.

Yb_3S_4 is another compound with large γ value in the specific heat and semiconducting transport properties.[29,30] The specific heat measured in an applied magnetic field behaves similarly to $Ce_3Au_3Sb_4$. Conduction by magnetic polarons has been suggested in Ref. 29. However, magnetic order would make the polarons coherent at low T and reduce the resistivity, whereas experimentally, the resistivity increases like in other semiconductors. A resonating valence bond theory proposed [31] for materials with Th_3P_4 structure (space group $I4$-$3d$) is based on the possible frustration in the equilateral triangular structure of the Ce sites, which is also the case for $Ce_3Au_3Sb_4$. Our specific heat results with La-Ce dilution (see Fig. 5), however, show a large specific heat at low T even in the single impurity limit, indicating that frustration is not the underlying mechanism of this peak.

V. SUMMARY

In summary, we measured the magnetic susceptibility, the specific heat in zero field and in applied magnetic fields, resistivity, and magnetoresistance to study and understand the unique ground state of $Ce_3Au_3Sb_4$. Assuming that the corresponding La and Pr compounds are semiconducting, as suggested by data from polycrystalline samples, we assumed that $Ce_3Au_3Sb_4$ also has an intrinsic band gap. A simple model involving a valence band and a conduction band hybridized with the f level together with small disorder (leading to localization of in-gap states) is able to qualitatively explain most of the experimental results. We also studied the specific heat of La-diluted samples, which leads to the conclusion that the specific heat anomaly is a local effect. The model also provides a qualitative explanation for the pressure dependence of the resistivity. It suggests that the in-gap states in $Ce_3Au_3Sb_4$ have a nature different from those in $Ce_3Bi_4Pt_3$. The two compounds are isostructural with very similar lattice constants. However, while $Ce_3Bi_4Pt_3$ is an ordinary Kondo insulator (hybridization gap) with in-gap states possibly due to excitonlike bound states,[32] $Ce_3Au_3Sb_4$ is gapped because $La_3Au_3Sb_4$ is already a semiconductor or semimetal. The density of in-gap states also differs significantly by about 3 orders of magnitude for the two compounds.

The study of $Ce_3Au_3Sb_4$ provides important information on heavy-fermion-like behavior in insulating systems and further knowledge on Kondo insulators. For further verification of the existence of f-level states in the gap, Raman scattering and optical measurements would be useful and are currently in progress. Confirming the intrinsic nature of ground state of $La_3Au_3Sb_4$ and $Pr_3Au_3Sb_4$ single crystals (whether semiconductor or semimetal) is also an important task.

ACKNOWLEDGMENTS

We thank R. Singh, D. Cox, and J. Lawrence for valuable discussions. This work was supported by DMR-NSF 0433560 (H.O.L. and Z.F.) and NSF DMR-0600742 (C.L.C. and S.M.K.), and C.L.C. acknowledges Tyco Electronics Foundation for functional materials. Y.-J.J. acknowledges support from the NHMFL Schuller program and L.B. from the NHMFL in-house research program. P.S. acknowledges the support of DOE under Grant No. DE-FG02-98ER45707. V.A.S. acknowledges the support from RFBR under Grant No. 06-02-16590 and Program "Physics of Strongly Compressed Matter" of the Presidium of Russian Academy of Sciences. Work at Los Alamos was performed under the auspices of the U.S. Department of Energy, Office of Science.

[1] A. C. Hewson, *Kondo Problem to Heavy Fermions* (Cambridge University Press, Cambridge, England, 1993).
[2] G. Aeppli and Z. Fisk, Comments Condens. Matter Phys. **16**, 155 (1992).
[3] J. W. Allen, R. M. Martin, B. Batlogg, and P. Wachter, J. Appl. Phys. **49**, 2078 (1978).
[4] T. Takabatake, F. Teshima, H. Fujii, S. Nishigori, T. Suzuki, T. Fujita, Y. Yamaguchi, J. Sakurai, and D. Jaccard, Phys. Rev. B **41**, 9607 (1990).
[5] M. F. Hundley, P. C. Canfield, J. D. Thompson, Z. Fisk, and J. M. Lawrence, Phys. Rev. B **42**, 6842 (1990).
[6] M. Kasaya, K. Katoh, and K. Takegahara, Solid State Commun. **78**, 797 (1991).
[7] P. S. Riseborough, Adv. Phys. **49**, 257 (2000).
[8] K. Katoh and M. Kasaya, Physica B **186-188**, 428 (1993).
[9] M. Kasaya, K. Katoh, M. Kohgi, T. Osakabe, and N. Sato, Physica B **199&200**, 534 (1994).
[10] D. T. Adroja, B. D. Rainford, Zakir Hossain, E. A. Goremychkin, R. Nagarajan, L. C. Gupta, and C. Godart, Physica B **206&207**, 216 (1995).
[11] K. Katoh and M. Kasaya, J. Phys. Soc. Jpn. **65**, 3654 (1996).
[12] K. Takegahara and Y. Kaneta, Prog. Theor. Phys. Suppl. **108**, 55 (1992).
[13] S. Kimura, Y. Sato, F. Arai, K. Katoh, M. Kasaya, and M. Ikezawa, J. Phys. Soc. Jpn. **62**, 4174 (1993).
[14] S. Kimura, Y. Sato, F. Arai, M. Ikezawa, M. Kasaya, and K. Katoh, J. Phys. Soc. Jpn. **64**, 4278 (1995).
[15] A. Amato, Physica B **206&207**, 49 (1995).
[16] A. Amato, R. Feyerherm, F. N. Gygax, A. Schenck, M. Kasaya, T. Suzuki, S. Takagi, and A. Ochiai, Hyperfine Interact. **104**, 165 (1997).
[17] S. Broderick, V. Vescoli, B. Buschinger, W. Guth, O. Trovarelli, M. Weiden, L. Degiorgi, C. Geibel, and F. Steglich, Solid State Commun. **108**, 463 (1998).
[18] G. M. Sheldrick, SHELXTL-97, University of Göttingen, 1997.
[19] A. Eiling and J. S. Schilling, J. Phys. F: Met. Phys. **11**, 623 (1981).
[20] E. Kaldis and P. Wachter, Solid State Commun. **11**, 907 (1972).
[21] A. V. Ryabov, B. I. Smirnov, S. G. Shul'man, T. B. Zhukova, and I. A. Smirnov, Sov. Phys. Solid State **19**, 1580 (1978).
[22] G. F. Chen, K. Matsubayashi, S. Ban, K. Deguchi, and N. K. Sato, Phys. Rev. Lett. **97**, 017005 (2006).
[23] J. C. Cooley, M. C. Aronson, and P. C. Canfield, Phys. Rev. B **55**, 7533 (1997).
[24] J. D. Thompson, W. P. Beyermann, P. C. Canfield, Z. Fisk, M. F. Hundley, G. H. Kwei, R. S. Kwok, A. Lacerda, J. M. Lawrence, and A. Severing, in *Transport and Thermal Properties of f-Electron Systems*, edited by G. Oomi (Plenum, New York, 1993), p. 35.
[25] T. Suzuki, Physica B **186**, 347 (1993), and references therein.
[26] K. Fraas, U. Ahlheim, P. H. P. Reinders, C. Schank, R. Caspary, F. Steglich, A. Ochiai, T. Suzuki, and T. Kasuya, J. Magn. Magn. Mater. **108**, 220 (1992).
[27] U. Ahlheim, K. Fraas, P. H. P. Reinders, F. Steglich, O. Nakamura, T. Suzuki, and T. Kasuya, J. Magn. Magn. Mater. **108**, 213 (1992).
[28] S. Takagi, H. Suzuki, A. Ochiai, T. Suzuki, A. Amato, R. Feyerherm, F. N. Gygax, and A. Schenck, Physica B **186-188**, 422 (1993).
[29] Y. S. Kwon, Y. Haga, C. Ayache, T. Suzuki, and T. Kasuya, Physica B **186-188**, 605 (1993).
[30] M. H. Jung, T. Park, H. J. Lee, and Y. S. Kwon, J. Korean Phys. Soc. **32**, 71 (1998).
[31] V. Y. Irkhin and M. I. Katsnelson, Phys. Lett. A **150**, 47 (1990).
[32] P. S. Riseborough, Phys. Rev. B **68**, 235213 (2003).